Quantization of a Free Particle Interacting Linearly with a Harmonic Oscillator

Thomas Mainiero

Abstract

We study the quantization of a free particle coupled linearly to a harmonic oscillator. The classical system, which has clearly separated chaotic and regular regions, is ideal for studies of the quantization of mixed systems. In this work, we detect signatures of chaos in the quantum system by investigating properties such as avoided crossings of eigenvalues as the coupling parameter is varied. We also study Husimi distributions to compare the quantum dynamics to phase portraits of its classical counterpart. These comparisons help in identifying key signatures of the classically chaotic/regular portions in the quantum system.

This paper examines the quantization of a free particle linearly coupled to a harmonic oscillator. Unlike generic mixed systems, the phase portrait of the classical system has clearly separated regular and chaotic regions, making its quantization ideal for studying the quantization of systems with mixed dynamics. By examining avoided level crossings and Husimi distributions, we demonstrate that as the chaotic fraction of classical phase space increases, the overall Husimi structure becomes mixed and delocalized.

1 Introduction

In recent decades, there has been a great deal of research on dynamical systems that do not follow regular and predictable patterns. In classical mechanics, such "chaotic" systems have well-defined trajectories, but they are extremely sensitive to their initial conditions (i.e., nearby trajectories can diverge exponentially). Extensive studies of such systems have opened new doors in understanding the natural world, as most systems exhibit chaotic dynamics rather than the simple regular behavior typically studied in the classroom.

However, it is not clear how to understand the notion of chaos in quantum mechanics. Wavefunctions evolve linearly in time. Hence, sensitive dependence on initial conditions and exponentially diverging trajectories–key components for defining classical chaos–cannot be used to define quantum chaos. Nevertheless, identifying features of quantum analogues of classically chaotic systems exist, so that they can be distinguished from quantum analogues of integrable (regular) systems.[1–4] The study of such identifying features using carefully chosen examples enables one to better understand the manifestations of chaos in quantum systems.

2 The Classical System

The interaction of two of the simplest quantum systems, the one-dimensional free-particle and the one-dimensional harmonic oscillator, arises in studies of dissipation in Hamiltonian systems, electron-phonon interactions in solids, and quantum decoherence.[5] Recently, De Bièvre, Parris, and Silvius, analyzed the classical counterpart of this system as a first step toward understanding its quantization.

These authors considered a classical particle of mass m, position $x(t)$, and momentum $p_0(t)$ moving on a ring divided into two sections. In one section (of length L) the particle is free and in the other (of length 2σ) the particle interacts with a harmonic oscillator of mass M, position $X(t)$, momentum $P(t)$, and frequency ω. The classical Hamiltonian is

$$H = \frac{{p_0}^2}{2m} + \frac{P^2}{2M} + \frac{1}{2}M\omega^2 X^2 - F_0 X\rho(x), \quad (1)$$

where F_0 describes the strength of the interaction, which is linear in X. The quantity $\rho(x)$ determines the range of the interaction: $\rho(x)$ is unity on the region $|x| \leq \sigma$ and zero when $|x| \in (\sigma, \sigma + \frac{L}{2})$. In non-dimensional form, Equation (1) is

$$H = \frac{1}{2}\left(p^2 + \Pi^2 + \Phi^2\right) - \alpha\Phi\chi(q), \quad (2)$$

where p and Π are, respectively, the particle and oscillator momenta, q and Φ are the particle and oscillator coordinates, α is the particle-oscillator coupling parameter, and $\chi(q)$ is a function that is unity in the interaction region and vanishes elsewhere. Here the interaction region and uncoupled regions are respectively defined by $q \in [-1, 1]$ and $q \in (1, 2+L)$; so the length of the uncoupled region is L. The only system parameters that can be varied are α and L.

The equations of motion resulting from (2) are

$$\dot{q} = p, \qquad \dot{p} = \alpha\Phi[\delta(q+1) - \delta(q-1)], \quad (3)$$
$$\dot{\Phi} = \Pi, \qquad \dot{\Pi} = -\Phi + \alpha\chi(q),$$

where dots denote time derivatives. Equation (3) indicates that the particle behaves freely in both the interaction and free regions. The classical dynamics become interesting when the particle arrives at boundaries between the two regions (i.e., when $q = \pm 1$). Here, the particle reaches a potential barrier of height $\pm\alpha\Phi$, where the sign depends on whether it is coming from the interaction region (+) or the free region (−). The particle bounces off the boundary elastically if its kinetic energy p^2 is less than the barrier height; otherwise, it overcomes the barrier and enters the new region with a kinetic energy of $p^2 \mp \alpha\Phi$. Because the barrier height depends on the oscillator coordinate Φ, it is easy to see how the dynamics can become complicated.

A particularly interesting facet of this system is the clean separation of integrable and chaotic regions in its phase space. Phase portraits of the oscillator coordinate and momentum possess an integrable region for system energies varying from the ground state energy $E_g = -\frac{{F_0}^2}{2M\omega^2}$ to a critical positive energy $E_c = |E_g|$. However, for small positive energies outside this region, the motion appears to be fully chaotic without any additional KAM structures near the boundary between the two regions.[5] The clean separation helps simplify comparisons between the classical and quantum system and makes the present example a very illuminating one. Such simple comparisons are not possible for generic systems with mixed dynamics, as they possess a hierarchy of KAM structures with intricately mixed chaotic and integrable regions. This could lead to great insights in quantum chaotic systems and, in particular, the quantization of mixed systems; this is the main motivation in this paper.

3 The Quantum System

Using the canonical quantization procedure (see Appendix I), we arrive at the quantization of (2):

$$H = \frac{1}{2}\left(-\frac{\partial^2}{\partial q^2} - \frac{\partial^2}{\partial \Phi^2} + \Phi^2\right) - \alpha\Phi\chi(q) \quad (4)$$

For the uncoupled case ($\alpha = 0$), the time-independent Schrödinger equation $H|\psi\rangle = E|\psi\rangle$ is separable; the problem reduces to determining the eigenstates of the harmonic oscillator and the free particle confined to a ring of length $2 + L$ as separate problems. The exact solutions for these two problems can be easily obtained. If $\{|\psi_k^{part}\rangle\}_{k=0}^{\infty}$ and $\{|\psi_l^{osc}\rangle\}_{l=0}^{\infty}$ are eigenstates of the particle and the harmonic oscillator, respectively, then $\{|\psi_k^{part}\rangle \otimes |\psi_l^{osc}\rangle\}_{k,l=0}^{\infty}$ are eigenstates for the uncoupled system[†]. In fact, these states form a basis for the Hilbert

[†]Formally, $|\psi_k^{part}\rangle \otimes |\psi_l^{osc}\rangle$ is an element of the tensor product space $\mathcal{H}_{part} \otimes \mathcal{H}_{osc}$, where $\mathcal{H}_{part}$ and $\mathcal{H}_{osc}$ are the particle and oscillator Hilbert spaces, respectively. Readers unfamil-

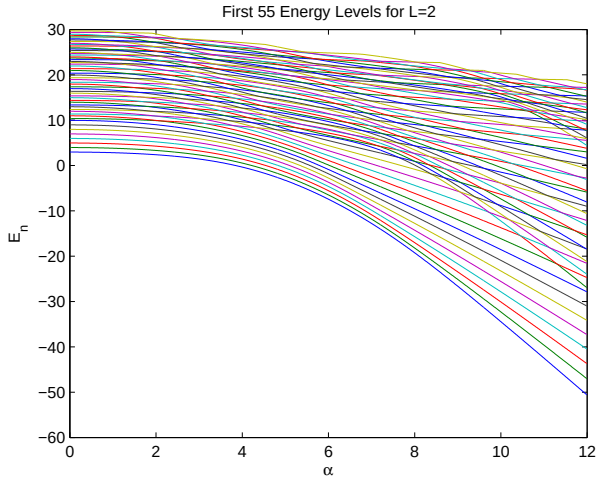

Figure 1: The first 55 energy levels as a function of α for Equation (4) with uncoupled region length $L = 2$. This plot was calculated using a 2025×2025 truncated Hamiltonian matrix.

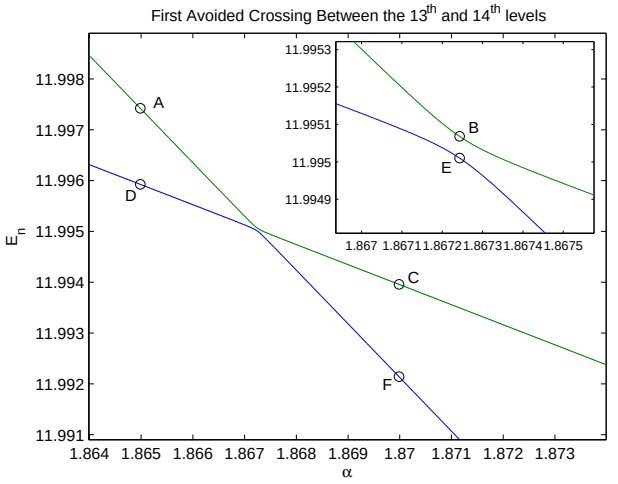

Figure 2: Avoided crossing of the 13^{th} and 14^{th} levels with $L = 2$. The inset shows a magnification of the avoided crossing. Labels designate where Husimi distributions are calculated and displayed in Figure (see Section 5 and Figure 7)

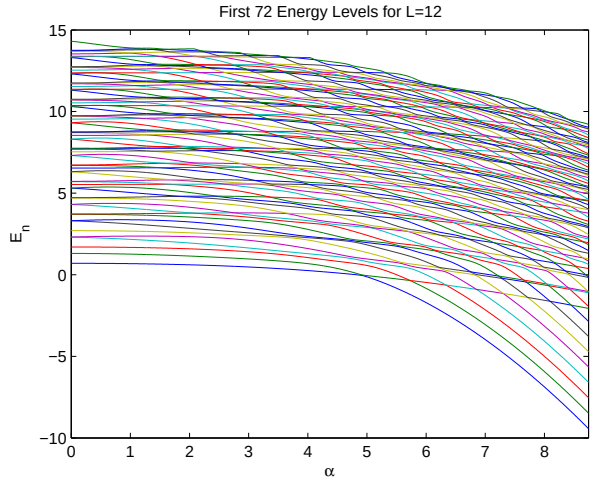

Figure 3: The first 72 energy levels as a function of α for Equation (4) with uncoupled region length $L = 12$. This plot was calculated using a 4900×4900 truncated Hamiltonian matrix.

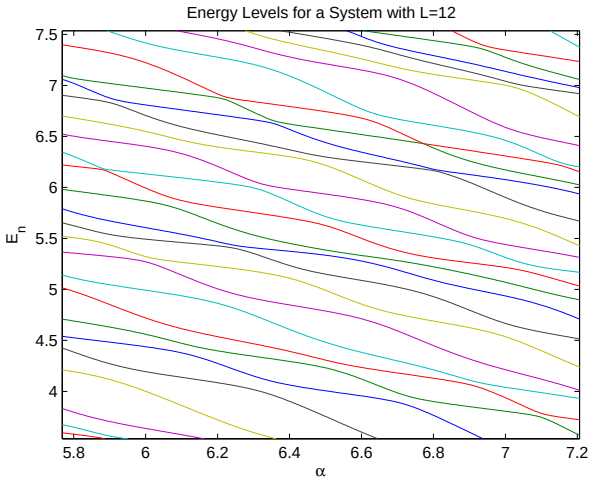

Figure 4: Broad avoided crossings between levels for Equation (4) with $L = 12$.

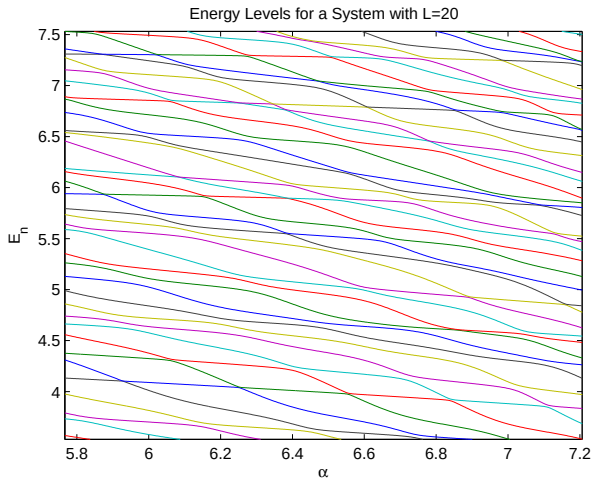

Figure 5: Broad avoided crossings between levels for a system with $L = 20$. Note the increased density of energy levels and avoided crossings compared to Figure 4.

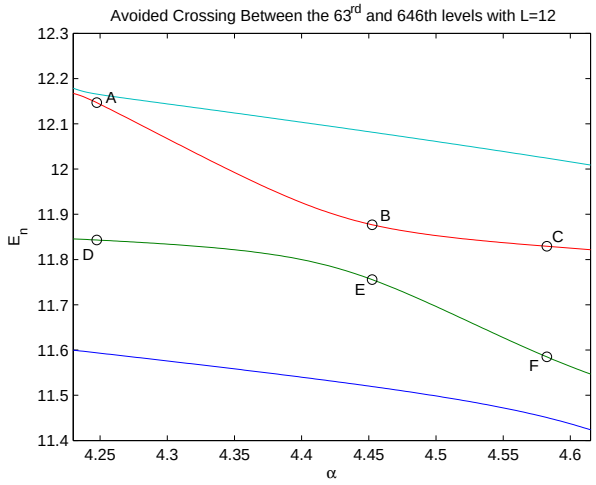

Figure 6: Broad crossing between the 63^{rd} and 64^{th} levels. Here the 62^{nd} and 61^{st} levels are shown as upper and lower bounds, respectively. Note that the 63^{rd} level begins to come into a broad avoided crossing with the 62^{nd} level before it totally exchanges slope from its previous encounter. Labels designate where Husimi plots are calculated and displayed in Figure 8.

space of either the coupled or uncoupled system. By representing the Hamiltonian (4) as an infinite matrix using this basis (see Appendix II), we can approximate the eigenvalues and eigenstates by finding the eigenvalues and eigenvectors of a truncation of the matrix.

4 Avoided Crossings

As the coupling parameter α is varied, the eigenvalues of (4) may come very close to one another or even cross. If the Hamiltonian is invariant under a symmetry transformation[‡] for a certain range of α, it can be block-diagonalized by exploiting this symmetry[§]. Energy levels belonging to different blocks can cross as α is varied.[3,4,6] On the other hand, if a quantum Hamiltonian has no symmetries other than time reversal, then such a level crossing is called an "accidental degeneracy" and requires two arbitrary parameters to exactly coincide.[4] In this case, most levels that approach another level end up avoiding one another instead of crossing.

Classically chaotic systems have fewer constants of motion than degrees-of-freedom and thus usually have fewer symmetries than integrable systems with the same degrees-of-freedom. Similarly, one expects the quantization of a classically chaotic system to possess fewer symmetries than degrees-of-freedom.[7,8] Thus, for the quantization of a chaotic system, one expects fewer level crossings to than for the quantization of an integrable system. Hence, an abundance of avoided crossings between levels may be a signature of chaotic regions in the classical system.

Figure 1 shows the first fifty-five energy levels as a function of α in a system with $L = 2$ using an α-

iar with the tensor product may think of $|\psi_k^{prt}\rangle \otimes |\psi_l^{osc}\rangle$ in terms of its coordinate-space wavefunction $\psi_k^{part}(q)\psi_l^{osc}(\Phi) = \langle q, \Phi|\{|\psi_k^{part}\rangle \otimes |\psi_l^{osc}\rangle\}$ or appeal to the references.[26]

[‡]The Hamiltonian is invariant under a symmetry transformation S if $[H, S]$=0.

[§]We do this by choosing each block to be invariant under the symmetry transformation. In physical situations, a continuous symmetries may correspond to a conserved quantity by Noether's theorem.[9]

step size [†] of 2.5×10^{-3}. Apparent level crossings seem to occur along smooth curves which appear as "light" regions in Figure 1. Refining the numerical computation at some of the apparent crossings on these curves shows that these are actually avoided crossings in which the slopes of the energy level curves are exchanged. Avoided crossings of this nature are described as "sharp" avoided crossings.[4,10] Through such crossings, the participating levels act as if they have entered a level crossing, merely exchanging their eigenstates.[6] We have verified this numerically for our system (see the Section 5), and this has also been noted in other systems such as a sinusoidally driven particle in a square potential well[10] and a hydrogen atom under strong magnetic fields.[11]

Figure 2 displays the first avoided crossing between the 13^{th} and 14^{th} levels in Figure 1 using the refined α-step size 7.5×10^{-6}. In general, the α-step size at which the avoided crossings in Figure 2 can be resolved is $O(10^{-6})$. As a result, it is time-consuming to numerically verify that all of the apparent crossings are actually very sharp avoided crossings. However, the coupled Hamiltonian seems to possess no physically obvious symmetries other than time-reversal[‡]. Assuming this is true, level crossings would be accidental degeneracies, which are rare (see the discussion above). Rigorously proving the Hamiltonian has no other symmetries is a difficult problem in general.[12]

Another notable feature of Figure 1 is that relatively smooth, widely-spaced energy curves form the first nine levels. This is unsurprising, as in the uncoupled system with $L = 2$, the first nine levels of the oscillator have less energy than the ground-state of the particle. This gives the levels of the system their wide spacing, which is preserved as α increases. The wide spacing prevents as many avoided crossings between these levels as one observes for higher levels. As L increases, however, the ground-state energy of the particle drops quadratically in L and one would not expect this behavior to hold.

Figure 3 displays the energy curves of the first seventy-two levels with $L = 12$. Our numerical computations verify that the smooth nature of the first few levels is increasingly destroyed as L grows. Of greater interest, however, are the much broader avoided crossings, which become more prevalent as α increases . Figure 4 shows energy curves for $\alpha \in (5.6, 7.2)$; the α-step size in which this figure's avoided crossings can be resolved is $O(10^{-3})$, One-hundred times larger than the α-step size required to resolve the sharp avoided crossings in Figure 1. These broader avoided crossings make it more difficult to identify patterns of their occurrence, as with the "light" regions in Figure 1. In most of the broader avoided crossings, the energy curves are unable to exchange slopes completely before they meet another avoided crossing. Hence, one would not necessarily expect a complete exchange of eigenstate structure for these avoided crossings. Indeed, a study of such crossings for a sinusoidally driven particle in a square potential well shows a superposition of eigenstate structure in "broad" avoided crossings rather than a complete exchange;[10] we will refer to such a superposition as mixing.

Figure 5 displays the energy curves for a system with $L = 20$ using the same window as in Figure 6. Note the increased density of levels and broad avoided crossings. Because of this, it is more likely that a level in an avoided crossing will encounter another before slopes are completely exchanged. As the ground-state energy of the free particle is proportional to $1/(2+L)^2$, the density of levels in the ground-state should increase with L. Hence, as long as this increased density is loosely preserved with α (which seems to hold in our numerical computations), then one would expect more broad avoided crossings with increasing L.

5 Husimi Distributions

5.1 Introduction

Although there is no equivalent of classical phase space trajectories in quantum mechanics, there are

[†] The α-step size is the distance between successive values of α where eigenvalues and eigenvectors are calculated. The α-step size required to resolve sharp avoided crossings such as in Figure 2 is $O(10^{-6})$

[‡] All symmetries of the uncoupled Hamiltonian are broken: there is no parity and $[H, p] \neq 0$ for $\alpha \neq 0$.

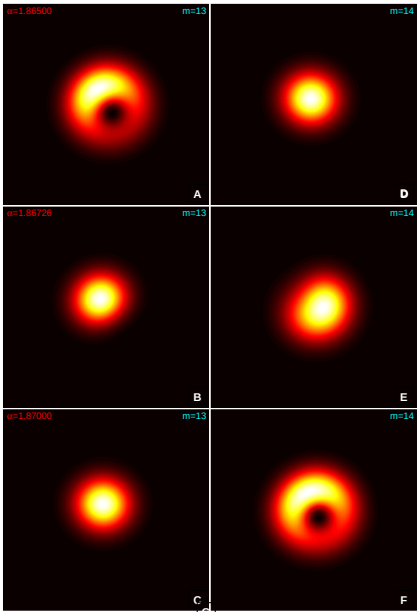

Figure 7: Husimi plot structure exchange through the sharp avoided crossing displayed in Figure 2. The left and right columns are the Husimi plots of the 13^{th} and 14^{th} levels, respectively. Π is on the vertical axis and Φ on the horizontal axis. Lighter regions correspond to higher probabilities.

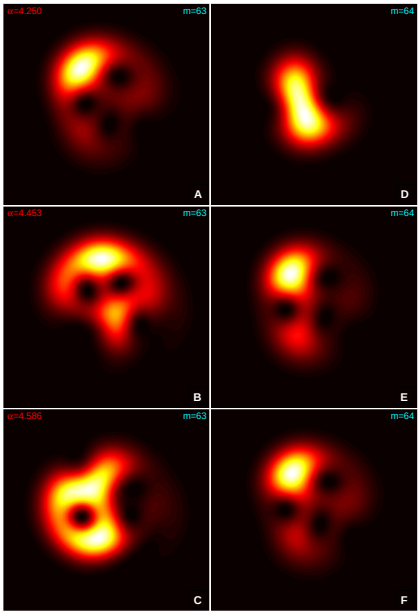

Figure 8: Husimi plot mixing through the broad avoided crossing displayed in Figure 6. The left and right columns are the Husimi plots of the 63^{rd} and 64^{th} levels, respectively.

suitable analogues. In particular, the Husimi distribution is often used in the study of quantum chaos.[2] Given a quantum state $|\psi\rangle$, its Husimi distribution $H_\psi(p,q)$ is defined by the projection of $|\psi\rangle$ onto a coherent state $|\psi_{(p,q)}\rangle$ localized around (p,q) so that $H_\psi(p,q) \propto |\langle\psi_{(p,q)}|\psi\rangle|^2$. For a system with a Euclidean topology, a coherent state localized at (p,q) is a Gaussian state whose position-space representation is localized around q and whose momentum-space representation is localized around p. The system possesses a cylindrical phase space topology[†]. We construct the coherent state for this topology from the Euclidean coherent state[13] (see Appendix III).

Coherent states provide excellent quantum analogues of classical particles when visualized as wave-packets that minimize the position-momentum uncertainty product[‡]. The projection onto these particle-like states thus can be viewed intuitively as a sort of classical smearing. The Husimi distribution is then interpreted as a probability distribution in phase space,[15] so that it provides a quantum analogue of a phase portrait. Determining the Husimi distribution for the eigenstates of a particular Hamiltonian thereby allows one to understand the dynamics of a quantum system in an analogous way to phase portraits its classical counterpart. The references provide a rigorous definition of the Husimi distribution,[15] as well as various applications.[15–18]

[†]In (4), $p \in \mathbb{R}$ and $q \in (2+L)\mathbb{S}^1$, where $\mathbb{S}^1$ is the unit circle. This gives a phase space [(p,q)-space] topology of $(2+L)\mathbb{S}^1 \times \mathbb{R}$, which is a cylinder.

[‡]For a one-dimensional system with position x and momentum p, the Gaussian wave-packet minimizes the product $\Delta x \Delta p$.

5.2 Exchange and Mixing of Husimi Structure at Avoided Crossings

5.2.1 Sharp Avoided Crossings

The Husimi distributions for the 13^{th} and 14^{th} eigenstates are depicted in Figure 7. The sequence of plots shows the change in their structure as the two eigenstates encounter the avoided crossing in Figure 2. The middle panels are snapshots near the closest point of the encounter. Note that the plots seem to be in the midst of exchanging the zero from the 13^{th} to the 14^{th} eigenstate and appear to be a superposition of the structures of the initial Husimi plots. The bottom panels, taken further away from the encounter, show that the two eigenstates have almost completely exchanged their structure through the avoided crossing. This is an example of the "exchange of character" in a sharp avoided crossing described above, which has also been observed in other dynamical systems.[10,14] Movies of the encounters[†] reveal a smooth structural exchange.

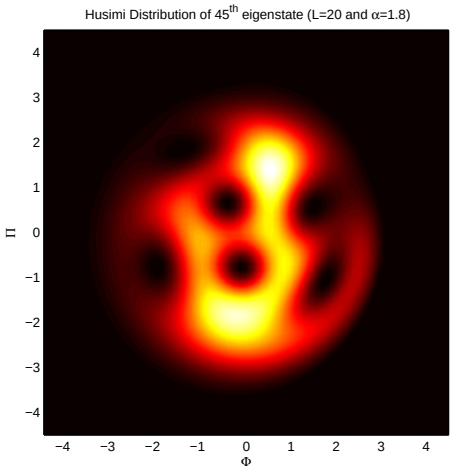

Figure 9: A highly delocalized Husimi distribution whose structure is spread throughout the available phase space and whose zeros do not lie on a smooth curve. The plot corresponds to a classical surface of section with a large chaotic region.

5.2.2 Broad Avoided Crossings

As described in Section 4, the energy curves in broad avoided crossings typically do not exchange slopes completely before another avoided crossing occurs. This generally leads to Husimi structure mixing,[10] rather than a complete exchange, which we have verified is the case for (4). Flr example, Figure 8 displays such a mixing between the 63^{rd} and 64^{th} levels in the avoided crossing from Figure 6. The exchange of structure is interrupted as the lower eigenstate encounters another avoided crossing. The levels clearly leave the crossing with Husimi structures that appear as a mix between the initial Husimi structures, rather than the exchange of initial structures depicted in Figure 7. Furthermore, this mixing causes the Husimi distribution of the 63^{rd} eigenvalue to delocalize after the avoided crossing. Thus, in contrast to sharp avoided crossings, broad avoided crossings play a significant role in modifying the overall Husimi structure as α increases;[10] in particular, broad avoided crossings seem to mix and delocalize the Husimi structure of individual eigenstates. Because broad avoided crossings tend to dominate the spectrum with increasing L, one expects the overall Husimi structure to depend more strongly on α for increasing L.

[†]These movies are available online at `http://www.its.caltech.edu/~mainiero/Husimimovies`.

6 Signatures of Chaos

As ergodicity and exponential divergence of phase space trajectories often characterize classically chaotic systems, it has been suggested that delocalization in the Husimi distributions of a quantum system is a possible signature of chaos in its classical counterpart.[19] This signature has been quantified and studied in numerical investigations[10,20] and is relevant as well for the system investigated here. The fraction of phase space with chaotic dynamics in the classical system (2) increases with L.[5] Thus, the delocalization and mixing of Husimi structures, which become more prominent as the number of broad avoided crossings increases with L, seem to be signatures of

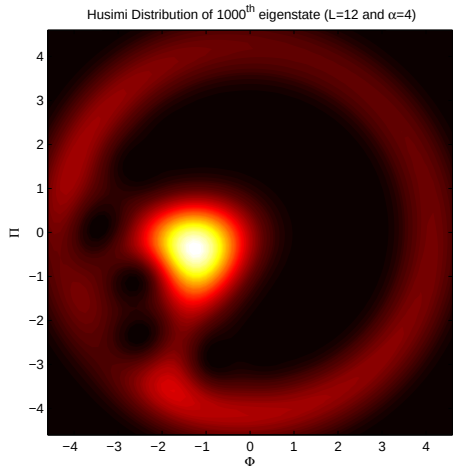

Figure 10: A Husimi distribution displaying anti-scarring as it localizes around an integrable region in Figure 13

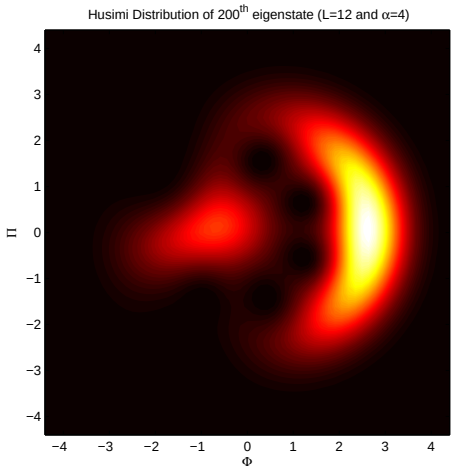

Figure 11: A Husimi distribution displaying both scarring and anti-scarring on the features of Figure 13.

this observation in the classical system.

6.1 Localization around Classical Features

The Husimi structure of a quantized system is often compared to corresponding classical Poincaré surfaces of section in order to detect the impact of chaotic and integrable features on the quantized system.[10,15,16] One manifestation is scarring (anti-scarring), in which an eigenstate tends to localize around unstable (stable) periodic orbits.[2] Also of interest are the zeros of the Husimi distribution. For states localized mainly in integrable regions, the zeros usually lie along smooth curves, while functions localized on chaotic regions usually have zeros dispersed almost uniformly throughout the available phase space.[23–25]

Figure 9 shows the Husimi distribution of the 45^{th} eigenstate for (4) with $L = 20$ and $\alpha = 1.8$. The zeros seem to be dispersed uniformly throughout the plot rather than lying along smooth curves. Furthermore, the Husimi structure is distributed throughout the entire available phase space, so it is highly delocalized. Thus, this Husimi distribution corresponds to a classical surface of section such as Figure 12, where the available phase space is entirely chaotic, .

We observe anti-scarring in many Husimi distributions of (4); the Husimi structure tends to localize in the integrable region which exists for energies varying from $E_g = -\frac{{F_0}^2}{2M\omega^2}$ to $E_c = |E_g|$ (described in Section 1). Figure 10 shows such localization near the integrable region visible as the white region in the center of Figure 13. On the other hand, Figure 11 displays an example of both scarring and anti-scarring. The depicted Husimi structure is localized mainly around the unstable periodic orbits, which are visible as dark arcs in the right half of the classical surface of section. However, other portions of the structure localize around the integrable region in the center of Figure 13. Note that the zeros of Figures 10 and 11 lie along smooth curves, in contrast to the Husimi distribution corresponding to a completely chaotic phase space (see Figure 9).

7 Conclusions

In this paper, we examined the quantization of a system with mixed chaotic-regular dynamics: a one-dimensional free particle on a ring coupled to a

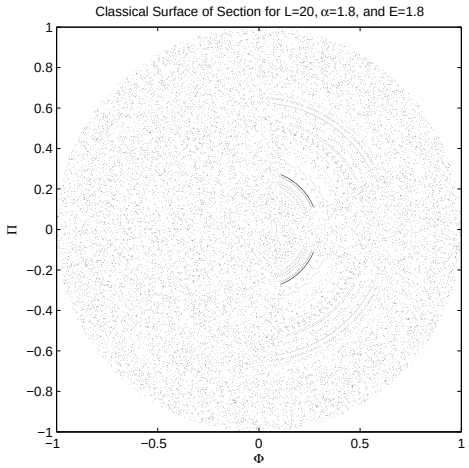

Figure 12: Classical surface of section with a large chaotic region for the same parameters L and α as the Husimi distribution in Figure 9. The dark arcs are unstable periodic orbits.

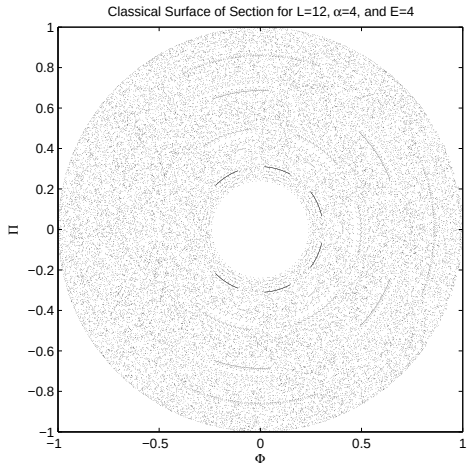

Figure 13: Classical surface of section with the same L and α as the Husimi distribution in Figure 9. The dark arcs are unstable periodic orbits.

one-dimensional harmonic oscillator. By examining eigenenergies as a function of the system parameters (coupling strength and the size of the uncoupled region) and Husimi distributions, we studied the quantum signatures of the mixed dynamics. We showed in particular that some apparent level crossings in the eigenenergies are actually very sharp avoided crossings and suggested why most (and perhaps all) other apparent crossings are also avoided crossings. We demonstrated numerically that the Husimi distribution structure between the two participating states in such crossings is completely exchanged.[6,10,14] This simple exchange helps preserve the overall Husimi structure as the coupling strength is varied.

As the size of the uncoupled region is increased, on the other hand, the avoided crossings broaden and their density increases. This increases the number of avoided crossings in which the participating energy curves do not fully exchange slope before encountering another avoided crossing. We show numerically that such broad avoided crossings mix the Husimi structure between participating states rather than exchange them fully as in the sharp avoided crossings observed more frequently when the uncoupled region is small. Such mixing tends to promote delocalization in the eigenstates as the coupling strength increases and shows that the overall structure of phase space depends on the coupling strength. Hence, as the size of the uncoupled region increases so that the number of broad avoided crossings increase, this dependence becomes stronger. In the corresponding classical system, the chaotic portion of phase space increases with the size of the uncoupled region. Thus, the appearance of broad non-adiabatic crossings, eigenstate delocalization, and the mixing of overall phase space structure seem to be signatures of chaos in the quantum system.

Acknowledgments

The author would like to acknowledge Mason Porter for continual help and direction, Alex McCauley for vital information and inspiration, and Stephen De Bièvre, Paul Parris, and Alex Silvius for their response to questions about their paper.[5] This research was funded by the Caltech Summer Under-

graduate Research Fellowship (SURF) Program and the Richter Memorial Funds.

Appendix I: Canonical Quantization

In this paper we use the canonical quantization procedure found in introductory quantum mechanics texts.[26,27] We assume the particle and oscillator act as bosons with no internal degrees-of-freedom and impose the following commutation relations:

$$\begin{aligned} [p,q] &= i, & [p,\Pi] &= 0, \\ [\Pi,\Phi] &= i, & [q,\Phi] &= 0, \\ [p,\phi] &= 0, & [\Pi,q] &= 0. \end{aligned} \tag{5}$$

We also use the coordinate-space identifications

$$p = -i\frac{\partial}{\partial q} \qquad \Pi = -i\frac{\partial}{\partial \Phi}. \tag{6}$$

This yields Equation (4),

$$H = \frac{1}{2}\left(-\frac{\partial^2}{\partial q^2} - \frac{\partial^2}{\partial \Phi^2} + \Phi^2\right) - \alpha\Phi\chi(q).$$

Appendix II: The Hamiltonian Matrix

Let $\mathcal{H}_1 = \mathcal{H}_{part}$ be the Hilbert space for a free particle constrained to a ring of length $2+L$ and $\mathcal{H}_2 = \mathcal{H}_{osc}$ be the Hilbert space for the uncoupled harmonic oscillator. Define $|n\rangle_1 = |\psi_n^{part}\rangle$ and E_n^1, respectively, as the n^{th} eigenstate and corresponding eigenenergy for this system. We calculate the coordinate projections $\{\psi_n^{part}(q)\}_{n=1}^{\infty}$ of $\{|n\rangle_1\}_{n=1}^{\infty}$ and their eigenenergies from the Schrödinger equation with periodic boundary conditions,

$$\begin{aligned} &\frac{\partial^2}{\partial q^2}\psi_n^{part}(q) = -E_n^1\psi_n^{part}(q), \\ &\psi_n^{part}(q + k(2+L)) = \psi_n^{part}(q),\ k \in \mathbb{Z}, \end{aligned}$$

which has the normalized solutions

$$\begin{aligned} \psi_n^{part}(q) &= \frac{1}{\sqrt{2+L}}\exp\left(-\frac{2\pi n}{2+L}i\right) \\ E_n^1 &= \frac{4\pi^2 n^2}{(2+L)^2} \end{aligned} \tag{7}$$

The ground state energy of the particle is $E_1^1 = 4\pi^2/(2+L)^2$.

Define $|k\rangle_2 = |\psi_k^{osc}\rangle$ and E_k^2 as the k^{th} eigenstate and corresponding eigenenergy, respectively. Here $E_k^2 = k + 1/2$ and $E_0^2 = 1/2$ is the ground-state energy.[26,27] (The coordinate projection for the eigenstates will not be given here, as it is easier to work with the abstract state vector $|k\rangle_2$.)

Using the operator definitions (6) in Appendix I, we write

$$a^\dagger = \frac{1}{\sqrt{2}}(\Phi - i\Pi), \qquad a = \frac{1}{\sqrt{2}}(\Phi + i\Pi),$$

which are the creation and annihilation operators, respectively, for the harmonic oscillator.[26,27] Equation (4) becomes

$$H = \left(a^\dagger a + \frac{1}{2}\right) - \frac{p^2}{2} - \frac{\alpha}{\sqrt{2}}\left(a^\dagger + a\right)\chi(q). \tag{8}$$

The matrix representation of (8) in the uncoupled basis $|n\rangle_1 \otimes |k\rangle_2{}_{n=1,k=0}^{\infty}$ is

$$\mathbf{H} = \mathbf{E_1} \otimes \mathbb{I} + \mathbb{I} \otimes \mathbf{E_2} - \alpha \mathbf{W_1} \otimes \mathbf{W_2}, \tag{9}$$

where $\mathbb{I}$ is the identity matrix and

$$\begin{aligned} (\mathbf{E_1})_{nn'} &= \langle n|\frac{-p^2}{2}|n'\rangle_1, \\ (\mathbf{E_2})_{kk'} &= \langle k|\left(a^\dagger a + \frac{1}{2}\right)|k'\rangle_2, \\ (\mathbf{W_1})_{nn'} &= \langle n|\chi(q)|n'\rangle_1, \\ (\mathbf{W_2})_{kk'} &= \langle k|\frac{1}{\sqrt{2}}\left(a^\dagger + a\right)|k'\rangle_2. \end{aligned}$$

By the definition of the uncoupled basis,

$$(\mathbf{E_1})_{nn'} = \frac{4\pi^2 n^2}{(2+L)^2}\delta_{nn'}, \tag{10}$$

$$(\mathbf{E_2})_{kk'} = \left(k + \frac{1}{2}\right)\delta_{kk'}. \tag{11}$$

Also, using the coordinate projections for the free particle eigenstates,

$$(\mathbf{W_1})_{nn'} = \int_0^{2+L} \psi_n^{part}(q)^* \psi_{n'}^{part}(q)\chi(q)\,dq = \int_0^2 \psi_n^{part}(q)^* \psi_{n'}^{part}(q)\,dq$$

Hence, with (7), we obtain

$$(\mathbf{W_1})_{nn'} = \begin{cases} \frac{1}{2\pi(n-n')}\left(-i + ie^{\frac{4\pi i(n-n')}{2+L}}\right) & \text{if } n \neq n', \\ \frac{2}{2+L} & \text{if } n = n'. \end{cases} \tag{12}$$

Finally, the creation/annihilation operator identities

$$a^\dagger|k\rangle_2 = \sqrt{k+1}|k+1\rangle_2, \quad a|k\rangle_2 = \sqrt{k}|k-1\rangle_2 \tag{13}$$

yield

$$(\mathbf{W_2})_{kk'} = \frac{1}{\sqrt{2}}\left(\sqrt{k'+1}\delta_{k,k'+1} + \sqrt{k'}\delta_{k,k'-1}\right). \tag{14}$$

Appendix III: The Husimi Distribution

The Husimi distribution $H_\psi(\bar{p},\bar{q},\bar{\Phi},\bar{\Pi})$ of a state $|\psi\rangle$ of the two-dimensional quantum mechanical system (4) is

$$H_\psi(\bar{p},\bar{q},\bar{\Phi},\bar{\Pi}) = N|\langle\psi_{(\bar{p},\bar{q},\bar{\Phi},\bar{\Pi}|)}|\psi\rangle|^2, \tag{15}$$

where $|\psi_{(\bar{p},\bar{q},\bar{\Phi},\bar{\Pi})}\rangle$ is a coherent state localized around $(\bar{p},\bar{q},\bar{\Phi},\bar{\Pi})$ and N is a normalization constant. We construct a coherent state for our system as

$$|\psi_{(\bar{p},\bar{q},\bar{\Phi},\bar{\Pi})}\rangle = |\psi_{(\bar{p},\bar{q})}\rangle_1 \otimes\ |\psi_{(\bar{\Phi},\bar{\Pi})}\rangle_2, \tag{16}$$

where $|\psi_{(\bar{p},\bar{q})}\rangle_1$ is the coherent state for the uncoupled particle and $|\psi_{(\bar{\Phi},\bar{\Pi})}\rangle_2$ is the coherent state for the uncoupled harmonic oscillator. The latter coherent state is[26,27]

$$|\psi_{(\bar{\Phi},\bar{\Pi})}\rangle_2 = e^{-\frac{1}{2}\left(\bar{\Phi}^2+\bar{\Pi}^2\right)}\sum_{k=0}^{\infty}\frac{\left(\bar{\Phi}+i\bar{\Pi}\right)^k}{\sqrt{k!}}|k\rangle_2. \tag{17}$$

Because $q \in (2+L)\mathbb{S}^1$ (i.e., the uncoupled particle system is $2+L$ periodic in q) and $p \in \mathbb{R}$, our phase space is cylindrical. We will use the procedure of Spina and Skodje[13] to define $|\psi_{(\bar{p},\bar{q},\bar{\Phi},\bar{\Pi})}\rangle$ for this topology. We require the coherent state $|\psi_{(\bar{p},\bar{q})}\rangle_1$ to satisfy

$$\langle q|\psi_{(\bar{p},\bar{q})}\rangle_1 = \langle q + k(2+L)|\psi_{(\bar{p},\bar{q})}\rangle_1,\ k \in \mathbb{Z}. \tag{18}$$

One can define the coherent states $|\psi_{(\bar{p},\bar{q})}\rangle_1$ using the Euclidean phase space coherent states $|\tilde{\psi}_{(\bar{p},\bar{q})}\rangle$ as

$$\langle q|\psi_{(\bar{p},\bar{q})}\rangle_1 = C^{\frac{1}{2}}\sum_{k=-\infty}^{\infty}\langle q + k(2+L)|\tilde{\psi}_{(\bar{p},\bar{q})}\rangle, \tag{19}$$

which satisfies (18) and converges because $\langle q + k(2+L)|\tilde{\psi}_{(p,q)}\rangle$ is Gaussian. In (19), C is a normalization constant to be determined by the condition $\langle\psi_{(\bar{p},\bar{q})}|\psi_{(\bar{p},\bar{q})}\rangle_1 = 1$.

The projection of $|\psi_{(\bar{p},\bar{q})}\rangle_1$ onto the uncoupled particle basis $\{|n\rangle_1\}_{n=1}^{\infty}$ is

$$\langle n|\psi_{(\bar{p},\bar{q})}\rangle_1 = \int_0^{2+L}\langle n|q\rangle_1\langle q|\psi_{(\bar{p},\bar{q})}\rangle_1\,dq = C^{\frac{1}{2}}\sum_{k=-\infty}^{\infty}\int_0^{2+L}\langle n|q+k(2+L)\rangle\times \times\langle q+k(2+L)|\tilde{\psi}_{(\bar{p},\bar{q})}\rangle\,dq.$$

The coordinate space projection of the Euclidean space coherent states is

$$\langle q|\tilde{\psi}_{(\bar{p},\bar{q})}\rangle = \left(\frac{1}{\pi}\right)^{\frac{1}{4}}\exp\left(-\frac{1}{2}\left(q-\bar{q}\right)^2 + i\bar{p}\left(q-\frac{\bar{q}}{2}\right)\right). \tag{20}$$

Because $\langle n|q+k(2+L)\rangle = \psi_n^{part}(q+k(2+L))$, using (7), (19), and (20) gives

$$\langle n|\psi_{(\bar{p},\bar{q})}\rangle_1 = C^{\frac{1}{2}}\left(\frac{1}{2}\right)^{\frac{1}{4}}\exp\left(-\frac{1}{2}\left(n-\bar{p}\right)^2 - i\bar{q}\left(n-\frac{\bar{p}}{2}\right)\right). \tag{21}$$

With the normalization condition $\langle\psi_{(\bar{p},\bar{q})}|\psi_{(\bar{p},\bar{q})}\rangle_1 = 1$, we determine from (21) that

$$C = \sqrt{\pi}\sum_{n=-\infty}^{\infty}e^{-(n-\bar{p})^2} \tag{22}$$

Thus, if a state $|\psi\rangle$ is expressed in the uncoupled basis $|n\rangle_1 \otimes |k\rangle_2{}_{n=1,k=0}^{\infty}$ as $|\psi\rangle = \sum_{n=1,k=0}^{\infty} a_{nk}|n\rangle_1 \otimes |k\rangle_2$, we obtain from (15),(17), and (21) that

$$H_\psi(\bar{p},\bar{q},\bar{\Phi},\bar{\Pi}) = \frac{C}{\sqrt{2}} \mid \sum_{n=1,k=0}^{\infty} a_{nk}^{*} \frac{\left(\bar{\Phi}+i\bar{\Pi}\right)^k}{\sqrt{k!}} \times$$
$$\times \exp\left(-\frac{1}{2}\left[\bar{\Phi}^2+\bar{\Pi}^2+(n-\bar{p})^2\right] - i\bar{q}\left(n-\frac{\bar{p}}{2}\right)\right) \mid^2 . \quad (23)$$

In practice, (23) is used as a truncated sum to determine the Husimi distribution for eigenstates calculated using a truncated Hamiltonian matrix for (4). To compare with the classical Poincaré sections, we take $\bar{q} = 1$ and $\bar{p} = \sqrt{2E - \bar{\Phi}^2 - \bar{\Pi}^2 - \alpha\bar{\Phi}}$ for an eigenstate with energy E. The first condition arises from a convention in choosing the Poincaré section for the classical system,[5] and the latter arises as a slice along the classical energy shell.

References

[1] Gutzwiller M. C. "Quantum Chaos" Scientific American, **266**, 78-84 (1992).

[2] Gutzwiller M. C. *Chaos in Classical and Quantum Mechanics*. New York: Springer-Verlag, 1990.

[3] Haake, Fritz. *Quantum Signatures of Chaos*. 2^{nd} ed. New York: Springer, 2001.

[4] Reichl, L. E. *The Transition to Chaos: Conservative Classical Systems and Quantum Manifestations*. 2^{nd} ed. New York: Springer, 2004

[5] De Bièvre S., Parris P. E, and Silvius A. "Chaotic Dynamics of a Free Particle Interacting Linearly with a Harmonic Oscillator," Physica D **208** (1,2), 96 (2005).

[6] von Neumann, J. and Wigner, E. Physik. Zeitschr. **30**, 465 (1929). English translation in: R.S. Knox and A. Gold, *Symmetry in the Solid State*. New York: W.A. Benjamin, 1964.

[7] Zhang, W., Martens, C., Feng, D., and Yuan, J. "Dynamical Symmetry Breaking and Quantum Nonintegrability," Phys. Rev. Lett. **61**, 2167 (1988).

[8] Zhang W., Feng, D., Yuan, J., and Wang, S. "Integrability and Nonintegrability of Quantum Systems: Quantum Integrability and Dynamical Symmetry," Phys. Rev. A **40** 438 (1989).

[9] Arnold, V. I. *Mathematical Methods of Classical Mechanics*. 2^{nd} ed. New York: Springer-Verlag, 1989.

[10] Timberlake, T., Reichl L.E., "Changes in Floquet-State structure at avoided crossings: Delocalization and harmonic generation," Phys. Rev. A **69** 2886 (1999).

[11] González-Férez, R. and Dehesa, J.S. "Characterization of atomic avoided crossings by means of Fisher's information," Eur. Phys. J. D **32** 39 (2005).

[12] Marsden, J.E. Private Communication 25 August 2006.

[13] Spina, A., Skodje, R. T., "The phase-space hydrodynamic model for the quantum standard map," Computer Phys. Comm. **63**, 279 (1991).

[14] Holder, B. P. and Reichl, L. E. "Avoided Crossings in Driven Systems," Phys. Rev. A **72**, 043408 (2005).

[15] Bäcker, A., Fürstberger, S., and Schubert, R. "Poincaré Husimi representation of eigenstates in quantum billiards," Phys. Rev. E **70**, 036204 (2004).

[16] Perotti L. "The Quantum Double Pendulum: A Study of an Autonomous Classically Chaotic Quantum System," Phys. Rev. E **70**, 066218 (2004).

[17] Chang, S. and Perez G., "Classical and Quantum Eigenstates of a Kicked Rotor," Chinese Journal of Physics **30** (4), 479 (1992).

[18] Chang, S. and Stuller, M. "The Quantum Kicked Rotor Revisited," Chinese Journal of Physics **35** (4) 469 (1997).

[19] Sugita, A. "Moments of generalized Husimi distributions and complexity of many-body quantum states," J. Phys. A **36** 9081 (2003).

[20] Sugita, A. and Aiba H. "Second moment of the Husimi distrubition as a measure of complexity of quantum states," Phys. Rev. E **65** 036205 (2002).

[21] Timberlake K.T. "What kind of research do you do in the Viking Center for Computational Physics?" VCCR Research. 22 Feb. 2006. `http://fsweb.berry.edu/academic/mans/ttimberlake/qchaos/work.html`.

[22] Lansel S., Porter M. A, and Bunimovich L.A. "One-Particle and Few-Particle Billiards," Chaos **16**, 013129 (2006).

[23] Leboeuf P. and Voros A. "Chaos-Revealing Multiplicative Representation of Quantum Eigenstates," J. Phys A: Math. Gen. **30** 1763 (1990).

[24] Leboeuf P. and Voros A. "Phase Space Approach to Quantum Dynamics," J. Phys. A: Math. Gen. **24** 4575 (1991).

[25] Korsch H.J., Müller, and Wiescher, H. "On the Zeros of the Husimi Distribution," J. Phys A: Math Gen. **30** L667 (1997).

[26] Cohen-Tannoudji, C., Diu, B., and Laloë, F. *Quantum Mechanics* Vol. 1. New York: John Wiley & Sons, 1977.

[27] Shankar, R. *Principles of Quantum Mechanics*. 2^{nd} ed. New York: Springer, 1994.

[28] P. Cvitanović, R. Artuso, R. Mainieri, G. Tanner, and G. Vattay, *Chaos: Classical and Quantum*, `ChaosBook.org` (Niels Bohr Institute, Copenhagen 2005).

[29] Wiggins, S. *Introduction to Applied Nonlinear Dynamical Systems and Chaos*. 2^{nd} ed. New York: Springer, 2003.